Tephra deposition enhances organic carbon burial in the Bering Sea

Jack Longman[1, 2, *] (ORCID: 0000-0002-2725-2617), Thomas M. Gernon[2] (ORCID: 0000-0002-7717-2092), Martin R. Palmer[2], Hayley R. Manners[2,3] (ORCID: 0000-0001-8545-4463).

[1]Marine Isotope Geochemistry, Institute for Chemistry and Biology of the Marine Environment (ICBM), University of Oldenburg, 26129 Oldenburg, Germany

[2]School of Ocean & Earth Science, University of Southampton, Southampton SO14 3ZH, UK

[3]School of Geography, Earth and Environmental Sciences, University of Plymouth, Plymouth, PL4 8AA, United Kingdom

[*] Corresponding author: Jack Longman: jack.longman@uni-oldenburg.de

Key Points

- Tephra layers are loci of organic carbon (OC) burial with distinct carbon isotopic composition.
- Preservation primarily linked to complexation of OC with reactive iron phases (accounting for ~80% of all OC in tephra layers).
- Distribution of reactive iron from tephra layers into surrounding sediment has enhanced OC burial in these layers (~33% of OC in sediments bound to reactive phases).
- OC-reactive Fe coupling observed in sediments >700,000 years old, which indicates the long-term persistence of these complexes.
- These interactions may help explain how labile OC may be preserved in sediments on long timescales.

Abstract

Preservation of organic carbon (OC) in marine sediments exerts a major control on the cycling of carbon in the Earth system. In marine sediment, OC preservation may be enhanced by diagenetic reactions in locations where deposition of tephra occurs. While the mechanisms by which this process occurs are well understood, site-specific studies are limited. Here, we report on a study of sediments from the Bering Sea (IODP Site U1339D) to investigate the effects of marine tephra deposition on carbon cycling during the Pleistocene and Holocene. Our results strongly suggest that tephra layers are loci of OC burial with distinct $\delta^{13}C$ values, and that this process is primarily linked to complexation of OC with reactive metals (accounting for ~80% of all OC within tephra layers). In addition, distribution of reactive metals into non-volcanic sediments above and below the tephra layers enhances OC preservation in these sediments, with ~33% of OC bound to reactive phases. Importantly, OC-Fe coupling is evident in sediments >700,000 years old. Thus, these interactions may help explain the preservation of labile OC in older marine sediments.

Plain Language Summary

The burial of organic carbon in marine sediments is one of the major carbon sinks in the oceans, meaning it acts to remove carbon dioxide from the ocean-atmosphere system. However, the speed at which burial occurs varies across the globe, dependant on a range of factors, from the amount of nutrients in the water, to the type of sediment. Despite evidence suggesting when tephra (or volcanic ash) is deposited to the seafloor carbon burial is enhanced, very little work has been done to investigate this process. We analysed sediments from the Bering Sea, where volcanoes from the Aleutian Islands and Kamchatka regularly deposit tephra in the ocean. We found that organic carbon burial is indeed associated with ash deposition, and that carbon is being preserved in the ash layers themselves. Our data indicate that this may be microbial carbon, related to organisms which use the nutrient-rich ash as a food source. We show here that this carbon is preserved effectively because of chemical reactions between the organic carbon and reactive iron, which is released by the ash, creating conditions which preserve carbon for a very long time.

1 Introduction

The preservation of organic carbon (OC) in marine sediments exerts a controlling influence on the carbon cycle, providing a link between the active pools (e.g. oceans, atmosphere and terrestrial environments) and the inactive, long-term carbon pools, such as those within sedimentary rocks (Arndt et al., 2013; Burdige, 2007; LaRowe et al., 2020). Only about 0.5% of all organic matter produced in the oceans is ultimately preserved in the sedimentary record, with the remainder remineralised and reintroduced into active carbon pools (Hedges & Keil, 1995). The process of OC burial and preservation leads to net removal of CO_2 from the atmosphere, thus any process which changes the marine sedimentary carbon sink is critically important for understanding the climate system (Burdige, 2007).

Explosive volcanism delivers roughly 1 km^3 of ash to the atmosphere every year (Pyle, 1995), and because a high proportion of volcanoes are located close to the oceans, much of this material falls into seawater and onto sea floor substrates (Olgun et al., 2011; Pyle, 1995). Tephra also enters the oceans through rapid erosion of newly created volcanic deposits (Cashman et al., 2013). This material eventually settles to the seafloor, and is deposited in the sedimentary record as tephra layers (Dingwell et al., 2012; Pyle, 1989). Tephra may also derive from submarine eruptions, such that tephra comprises as much as 25% of marine sediment in the Pacific Ocean (Scudder et al., 2009; Straub & Schmincke, 1998).

There are four mechanisms by which enhanced preservation of OC in marine sediments may occur as a result of tephra deposition and diagenesis: (1) fertilization; (2) reactive metal complexation; (3) reduced oxidant exposure, and (4) authigenic carbonate formation (Longman et al., 2019, 2020). Upon deposition into the ocean, and as a result of the dissolution of reactive mineral phases, tephra releases large amounts of macro and micronutrients such as P, Fe and Mn (Frogner et al., 2001; Jones & Gislason, 2008) that may alleviate deficiencies (Moore et al., 2013), particularly when Fe is the limiting nutrient. Indeed, the fertilization effect has been observed in the form of phytoplankton blooms in the aftermath of tephra deposition events (Achterberg et al., 2013; Duggen et al., 2010; Langmann et al., 2010; Uematsu et al., 2004). Tephra deposition on the seafloor rapidly reduces pore

water O_2 contents to near-zero as a result of oxidation of silicate-bound Fe^{II} (Haeckel et al., 2001; Hembury et al., 2012), thus inhibiting the oxidation and remineralization of OC.

Reactive metal complexation accounts for ~20% of all OC preserved in marine sediments (Lalonde et al., 2012), and it is known that reactive Fe, Mn and Al phases are released from tephra layers to adjacent sediments during diagenesis (Homoky et al., 2011). Hence, while it has yet to be directly observed it is likely that tephra deposition also contributes enhanced OC preservation through this process.

The association of abundant tephra layers and high OC concentrations has been taken to suggest that tephra diagenesis played a role in enhanced OC preservation in ancient environments (Lee et al., 2018; Tang et al., 2020), and there is growing evidence of tephra-related processes actively enhancing OC preservation in modern sediments (Hembury et al., 2012; Homoky et al., 2011; Murray et al., 2018; Wallmann et al., 2008). Nevertheless, the role of reactive metals released by tephra in this process has not been studied in detail.

Here, we estimate the contribution of this process (and the others outlined above) to the preservation of OC in the Bering Sea, and discuss the potential magnitude of these processes on a global scale. Our work investigates the changing chemistry above, below and within, tephra layers deposited throughout the Quaternary period to significantly improve our understanding of the impact tephra deposition has on the Earth system.

2 Methods and Materials

2.1 Study Site

Sediments from site U1339D IODP Expedition 323 (54°31.26'N, 169°44.35'W, 200 mbsl), on the Umnak Plateau in the Bering Sea (Fig. 1) largely comprise two lithological endmembers: biogenic diatom-rich sediment and a volcanogenic component. The volcanogenic material is sourced from eruptions along the Aleutian arc, and constitutes ~4 – 40% of the sediment (Takahashi, Ravelo, & Alvarez-Zarikian, 2011; Vaughn & Caissie, 2017). After visual identification of cores, subsampling of both tephra layers and background sediment was undertaken in this study. The surface of the split-

core sections was removed and care was taken to ensure that only the centre of the tephra layers was sampled to reduce contamination from the adjacent sediments below visibly detectable levels. For this study, we selected 9 sections, and for ease of understanding these are denoted Sections 1 to 9, and their depths and approximate ages are indicated in Figure 2 (see Supplementary Table 1 for details). Indicative ages were taken from the biostratigraphic age model of Takahashi et al. (2011b), interpolating linearly between the midpoint of each datum (see Fig. 2, Supplementary Table 1).

2.2 Geochemical Analyses

2.2.1 Organic Carbon

Organic carbon measurements were carried out on a Vario PYRO cube Element Analyser (EA) coupled to a vision isotope ratio mass spectrometer (IRMS) at the University of Southampton. Approximately 20 mg of homogenised sample was acidified in perchloric acid to remove any carbonate prior to multiple rinses with Milli-Q water. EA quality control was performed via repeated measurements of High Organic Sediment Standard (HOSS; Element Microanalysis Ltd.).

Bulk sediment carbon isotope signatures ($\delta^{13}C_{Bulk}$) were measured on CO_2 evolved from EA combustion, and calibrated to USGS 40 and USGS 41a, with reproducibility of ±0.02 ‰, and ±0.92 ‰, respectively (1 SD). Repeat analyses of HOSS (n=11), and Acetanilide (n=8) were used for quality control, with precision of ±0.04 ‰ and ±0.05 ‰ respectively (1 SD).

2.2.2 Inorganic Carbon

Approximately 20 mg of homogenised sediment was analysed via coulometry of evolved CO_2 after 10% perchloric acid addition, using an AutoMate Prep Device (AutoMate FX, Inc., Bushnell, Florida, USA) using a UIC CM5015 CO_2 Coulometer (UIC Inc., Joliet, Illinois, USA) at the University of Southampton. Calibration was performed using a pure carbonate standard (CAS #471-34-1), and quality control was completed via analysis of an in-house stream sediment standard.

Subsamples of layers which contained quantifiable levels of $CaCO_3$ were then selected for carbonate carbon and oxygen isotope analysis. According to the $CaCO_3$ content, between 5-15 mg of sample was analysed via a Thermo Scientific Kiel IV Carbonate device coupled to a MAT253 IRMS at the University of Southampton. Perchloric acid released CO_2, which was analysed for carbon and oxygen

isotopes ($\delta^{13}C_{Carb}$ and $\delta^{18}O$). Replicate analyses of an in-house standard were calibrated to NBS-18 and NBS-19, with reproducibility of ±0.13 ‰ and ±0.12 ‰ for $\delta^{13}C_{Carb}$, and ±0.17 ‰ and ±0.23 ‰ for $\delta^{18}O$ (1 SD).

2.2.3 Elemental Geochemistry

Bulk sample geochemistry was carried out after digestion at 130°C for 24 hours via a closed-vessel mixed acid (HNO_3-HCl-HF) approach. Digests were then diluted to 2% and analysed on a Thermo Scientific X-Series ICP-MS at the University of Southampton. Here, we present data for Al, Mn, Fe and Ba (Supplementary Table 1). Alongside samples, blanks and reference material (HISS-1 and JMS-1 marine sediment standards) were prepared and analysed in the same manner (see Supplementary Table 2 for HISS-1 recoveries and blank values).

2.2.4 Reactive Oxides

To isolate reactive oxide phases, a 4 hour dithionite extraction was performed (Kostka & Luther, 1994; Lalonde et al., 2012; Mehra & Jackson, 1958). For each sample, 4 ml of dithionite reagent (buffered to pH 4.8) was prepared, and added to 0.1 g of homogenised, freeze-dried sediment. To maintain pH 4.8, a buffered 0.35M sodium acetate, 0.2M sodium citrate solution was used, and heated to 60°C in a water bath. Samples were agitated using a vortex mixer every 15 minutes. This approach has been previously used to extract amorphous Fe-oxides alongside a fraction of crystalline Fe-oxides and acid volatile sulphides (Kostka & Luther, 1994; Roy et al., 2013). Dithionite-extracted fractions were diluted and analysed on a Thermo Scientific X-Series ICP-MS at the University of Southampton. Results are presented in Supplementary Table 3. Chilean Margin sediment (RR9702A-42MC, see Muratli et al., (2012)), was prepared and analysed in the same manner as the samples, with results for reactive Fe (Fe_R) and reactive Mn (Mn_R) found to be within the range of previously reported values (Supplementary Table 2). For Fe_R, values of 10475±125 ppm (1 SD, n=3) are close to previously measured values of 10800±800 ppm (Roy et al., 2013) and 9300±200 ppm (N.A. Murray et al., 2016). For Mn_R, measured values of 306±15 ppm (1SD, n=3) compare well with other studies, including 290±10 ppm (N.A. Murray et al., 2016), and 300±60 ppm (Roy et al., 2013) (Supplementary Table 2).

To investigate the composition of carbon associated with the phases extracted via dithionite leaching, we used the approach of Lalonde et al., (2012). This involves analysis of the OC content before and after the extraction experiment outlined above, and analysis of $\delta^{13}C_{bulk}$ before and after extraction. In addition, a control experiment was completed, where samples were extracted using sodium chloride instead of sodium dithionite and trisodium citrate, according to the method of Lalonde et al., (2012). For tephra, this released 0.004 wt% of the OC, and for sediment 0.02 wt%. These values were then used to correct experimental data (Lalonde et al., 2012; Shields et al., 2016), although it has been shown this approach can result in underestimations of Fe_R-associated OC (Fisher et al., 2020) (Supplementary Table 4). For simplicity, and in a similar manner to previous studies (e.g. Faust et al., 2021), we consider the results of the extraction experiment to represent Fe_R-bound OC, and not Mn_R- and Al_R-bound OC. Results are presented in Supplementary Table 4.

Using the results of the extraction experiment and control experiment, the fraction of OC associated with reactive phases (hereafter $f_{Fe\text{-}OC}$) and the isotopic composition of this OC (hereafter $\delta^{13}C_{Fe\text{-}OC}$) were calculated using the following equation (Lalonde et al., 2012):

$$f_{Fe-OC} = \frac{OC_{control} - OC_{extract}}{OC_{bulk}}$$

where $f_{Fe\text{-}OC}$ is the fraction of OC bound to reactive phases, $OC_{\text{-control}}$ is the OC content after control extraction (for either tephra or sediment), $OC_{\text{-extract}}$ is OC content after dithionite extraction and $OC_{\text{-bulk}}$ is OC content prior to extraction. The isotopic composition of the fraction of OC extracted ($\delta^{13}C_{Fe\text{-}OC}$) was calculated using the following equation:

$$\delta^{13}C_{Fe-OC} = \frac{\delta^{13}C_{bulk} \times OC_{bulk} - \delta^{13}C_{Fe-OC-extract} \times OC_{extract}}{OC_{bulk} - OC_{extract}}$$

where $\delta^{13}C_{bulk}$ is the $\delta^{13}C$ of OC before the dithionite experiment and $\delta^{13}C_{Fe\text{-}OC\text{-}extract}$ is the $\delta^{13}C$ of OC after the dithionite extraction. Using the calculated $\delta^{13}C_{Fe\text{-}OC}$, and the absolute amount of OC associated with Fe_R (OC_{Fe}), the isotopic composition of the non Fe_R-bound OC ($\delta^{13}C_{Non\text{-}Fe\text{-}OC}$) was then calculated using the following equation:

$$\delta^{13}C_{Non-Fe-OC} = \frac{\delta^{13}C_{Fe-OC} \times OC_{Fe} - \delta^{13}C_{bulk} \times OC_{bulk}}{OC_{Fe} - OC_{bulk}}$$

2.2.5 Palaeoproductivity

To assess changing palaeoproductivity, we used the biogenic fraction of barium (Ba_{Bio}), a commonly used proxy (Schoepfer et al., 2015). This approach first calculates the proportion of excess Ba in the sediments, an approach which uses the expected ratio of Ba to the conservative element Al in detrital, non-biogenic Ba to calculate the remainder:

$$Ba_{Bio} = Ba_{Total} - Al_{Total} \times \left(Ba / Al_{detrital}\right)$$

For $Ba/Al_{detrital}$, we assume the primary detrital contributor is tephra and use an average value from all tephra layers in this study (0.0099). Using published biostratigraphic ages (Takahashi, Ravelo, & Alvarez Zarikian, 2011), we calculate accumulation rates which are then used to convert raw Ba_{Bio} into Ba_{Bio} flux:

$$Ba_{Bio}Flux = Ba_{Bio} \times \rho \times LSR$$

where LSR is the linear sedimentation rate, in cm^{-1} kyr and ρ is the density of sediment, estimated using the following equation:

$$\rho = 0.0794 \times \ln(x) + 0.650$$

where x is the age of the sample in kyr (Schoepfer et al., 2015). Results may be found in Supplementary Table 1.

3 Results

The composition of the tephra layers and adjacent non-volcanogenic sediments are compared in Table 1. The tephra layers show lower average OC and inorganic carbon contents, but extend to much higher inorganic carbon concentrations in Section 6 (Fig. 2). The bulk $\delta^{13}C$ values of the two groups overlap, but the tephra layers have more negative mean $\delta^{13}C$ values (-25.4±1.18‰, 1SD, n=22) than the sediments (-23.91±0.6‰, 1SD, n=44) (Supplementary Table 5). The tephra layers are enriched in total Fe, Mn and Al, but contain slightly lower reactive phase contents (Fig. 3; Table 1). The

dithionite extraction experiment shows a greater average $f_{Fe\text{-}OC}$ in tephras (79±13%, 1SD, n=13) than sediments (33±22%, 1SD, n=24), with $\delta^{13}C_{Fe\text{-}OC}$ in tephras and sediments averaging -25.83‰ and -24.16‰, respectively (Table 1; Fig. 4, Supplementary Table 4). Carbonate $\delta^{13}C$ analyses show two clusters for $\delta^{13}C_{Carb}$ (Fig. 5). One cluster (n=5) displays a narrow range in $\delta^{13}C_{Carb}$ values between -1.01 and -1.58 ‰. The other (n=8) has $\delta^{13}C_{Carb}$ values between -13.41 and -19.56 ‰. $\delta^{18}O$ values also differ between the two clusters, with samples in the first lying between -7.09 and 1.34 ‰ and the second between 2.92 and 9.2 ‰ (Fig. 5).

4 Discussion

4.1 OC in tephra layers

Our analyses show that all tephra layers contain OC, with an average of 0.3 wt%, compared to an average of 0.9 wt% in the background sediments (Fig. 2a, Supplementary Table 5). Fresh tephra contains negligible OC, hence these data indicate that some OC preservation mechanism occurred within the tephra layers. Bulk carbon isotope analyses of the tephra layers and surrounding sediments indicate that the composition of this OC is different to what is preserved in surrounding sediments, with mean tephra $\delta^{13}C$ of -25.4±1.2‰ (1SD, n=22) and mean sediment $\delta^{13}C$ of -23.9±0.6‰ (1SD, n=44) (Fig. 2d). This suggests that the tephra layers contain a distinct source of ^{13}C-depleted carbon. It is possible this represents a shift to OC of a more terrestrial origin in tephras, with Yukon River OC typically ~-27‰ (Guo & Macdonald, 2006). However, this is unlikely to constitute a significant proportion of the OC supply to our site, with the Yukon delta nearly 1000 km to the northeast. In addition, there is no a priori reason to expect the tephra layers to contain more terrestrial OC than the sediments. Instead, we suggest the distinct OC $\delta^{13}C$ values in the tephra may be related to autochthonous microbial OC formation, because microbial fatty acid $\delta^{13}C$ values range from -30 to -45 ‰, depending on the carbon source (Cifuentes & Salata, 2001; Gong & Hollander, 1997; Hayes, 2001), meaning a relatively small contribution is necessary to result in the observed isotopic shift. Further study would be required to confirm this hypothesis, but evidence suggests volcanic glass may provide the ideal substrate for microbial growth (Li et al., 2020; Zhang et al., 2017). A number of studies have documented the existence of microbial communities which subsist on basaltic glass in

the upper oceanic crust (Fisk et al., 1998; Thorseth et al., 1995, 2001), with evidence of microbial alteration clear on glasses which are billions of years old (Staudigel et al., 2008). A final possibility is that the shift in lithology from sediment to tephra has allowed for the preferential preservation of certain compounds, due to changing reactivity and chemical composition. This could be linked to the preservation of OC via complexation with reactive iron (Fe_R) phases, as a result of the high Fe_R content in ash (Homoky et al., 2011), and evidence to suggest Fe release from tephra alteration (Luo et al., 2020; Maters et al., 2017).

4.2 Reactive metal complexation

Globally, ~20% of marine OC is thought to be preserved via complexation with Fe_R phases (Barber et al., 2017; Lalonde et al., 2012), hence we have investigated how complexation reactions may have influenced OC preservation at U1339D. The $f_{OC\text{-}Fe}$ in the background sediment (average 33%) is similar to the global average, but within the tephra layers, $f_{OC\text{-}Fe}$ increases to an average of 79% (Fig. 4; Table 1). By comparison, the highest $f_{OC\text{-}Fe}$ observed in marine sediments elsewhere is ~40% in deltaic sediments and ~30% in sediments underlying the equatorial Pacific upwelling zone (Lalonde et al., 2012). The intense Fe_R-OC complexation within the tephra layers may be linked to the high proportion of Fe^{II} within tephra deposits (Homoky et al., 2011), that provides an ideal environment for OC inner-sphere complexation (Barber et al., 2017). The higher proportion of $f_{OC\text{-}Fe}$ in the sediments adjacent to the tephra (relative to the more distal sediments) (Fig. 4) may be related to the diffusion of colloidal reactive Fe out of the tephra layers (cf. Homoky et al., 2011). Interestingly, the Fe_R content of the tephra layers at site U1339C is lower than in background sediments (Fig. 3), potentially because Aleutian eruptions are primarily andesitic and rhyolitic as opposed to basaltic (Supplementary Figure 1),

The isotopic signature of the Fe_R-bound OC ($\delta^{13}C_{Fe\text{-}OC}$) may indicate the type of OC being preserved via these interactions (Fig 4b, d, f). As with bulk $\delta^{13}C$, the $\delta^{13}C_{Fe\text{-}OC}$ of tephra layers is consistently more negative than in sediments, with an average of -25.50 ‰ in tephra and -22.4 ‰ in sediments (Fig. 4f), suggesting a distinct carbon source. The affinity of marine OC to Fe_R phases has been observed in a range of marine sediments located on the continental shelf previously (Lalonde et al.,

2012), and our findings are in line with those from other marine environments such as estuaries (Sirois et al., 2018; Zhao et al., 2018). As with bulk sediment OC, we believe this represents a shift toward microbial OC generation and preservation. Circumstantial evidence for this hypothesis comes from laboratory studies which demonstrate that reactive Fe oxides may act as electron suppliers for metabolism of metal-reducing bacteria (Coker et al., 2012; Kato et al., 2010). In contrast, in background sediments, $\delta^{13}C_{Fe\text{-}OC}$ displays less negative isotope ratios (Fig. 4). This suggests that outside of tephra layers, more typical marine OC such as phytoplankton debris is being preserved. The enhancement of microbial OC preservation due to Fe_R complexation in tephra layers may thus provide a previously unconsidered sink for such OC in sediments containing abundant tephra (J. I. Hedges et al., 1997).

The molar ratio of organic carbon to iron (OC:Fe; Fig. 5a, Supplementary Table 4) may yield information on the mechanisms of binding between OC and Fe (Faust et al., 2021; Lalonde et al., 2012), with low ratios indicative of simple mono-layer sorption, and higher ratios related to coprecipitation (Wagai & Mayer, 2007). In the Bering Sea sections, molar ratios vary greatly, suggesting a range of OC-Fe interactions, but tephra layers typically display lower OC:Fe than surrounding sediments (Fig. 5a). The high OC:Fe ratios observed in some sediment and tephras (OC:Fe >10) may indicate layers deposited under anoxic/sub-oxic conditions (Lalonde et al., 2012), in this case likely related to the consumption of porewater O_2 during tephra diagenesis (Hembury et al., 2012). Low OC:Fe ratios are typically linked to O_2 exposure (Lalonde et al., 2012), or terrestrial OC-Fe complexation (Barber et al., 2014; Faust et al., 2021), but as discussed above we believe neither of these mechanisms to be at play here. If microbial activity is a contributor to tephra OC, utilization of the reactive Fe during microbial metabolism may have altered the Fe_R content (Elizabeth Cooper et al., 2017; Eusterhues et al., 2014). Further, since the dithionite extraction removes all “reactive” Fe phases, and not simply those complexed with OC, it is possible that low OC:Fe ratios are related to the extraction of Fe_R phases not involved with complexation (Faust et al., 2021).

4.3 Long term persistence of an enhanced 'rusty sink' in tephra-rich sediments

Regardless of the source of the OC preserved in the sediments and tephra, there is evidence of extensive OC-Fe_R complexation in all layers of Bering Sea sediment, with particularly high levels of OC complexion in both the tephras and surrounding sediments (Fig. 4). These values suggest that the environment produced by tephra deposition, in which enhanced availability of nutrients (and especially Fe_R) is coupled to localised oxygen depletion (Hembury et al., 2012), is one in which high proportions of local OC are complexed to Fe_R. The enhanced $f_{OC\text{-}Fe}$ proportions in tephras are greater than reported in any surface sediments, even in anoxic depositional environments, suggesting the size of the 'rusty sink' in any given sediment may be more related to the availability of Fe_R phases and not the available oxygen (Lalonde et al., 2012).

In addition, even in the oldest layers around the tephra deposited between 700-745 kyr (i.e., section 21H4; Takahashi et al., 2011), all $f_{OC\text{-}Fe}$ proportions are above 10%, and greater than 70% in the tephra. This suggests that complexation with reactive oxides provides a long-term sink for OC in the marine environment, one which persists for far longer than previously indicated (Faust et al., 2021). This has implications for long-term carbon cycling on Earth, suggesting OC-Fe complexation may represent an important component of the high activation energy (*E*) OC involved in the long-term preservation of marine OC (Hemingway et al., 2019). The proportion of high-*E* organic compounds has been shown to increase as time proceeds in marine sediments, with our work suggesting a proportion of this is linked to OC-Fe_R complexation. This finding, coupled with the implication that tephras are loci of intense OC-Fe_R complexation, suggest that tephras may be involved in the burial and long-term sequestration of OC after periods of major volcanic activity, such as in the mid-Cretaceous (Lee et al., 2018) and in the Late Ordovician (Buggisch et al., 2010).

4.4 Other processes involved in OC preservation

Another potential carbon sink in tephra is authigenic carbonate (Schrag et al., 2013), which may form in tephra layers themselves, or sediments in which levels of Ca^{2+} and Mg^{2+} have been enhanced by ash deposition (Longman et al., 2019). In most tephras and sediments at site U1139D there is little evidence of this process occurring (Fig. 2b), but there are exceptions, particularly in one layer where

carbonate contents exceed 50 wt% (tephra 7; Fig. 2b). In addition, a small number of sediment layers show carbonate enrichment (Fig. 2b).

Carbon and oxygen isotope analyses of the carbonates ($\delta^{13}C_{Carb}$) indicate that there are two clear groups (Fig. 5b). The first, composed solely of carbonate from sediment layers, is characterized by $\delta^{13}C_{Carb}$ between -1 and -2 ‰, and appears to be indicative of a biogenic carbonate formation, or authigenic carbonates formed from dissolved inorganic carbon in seawater (e.g. Humphreys et al., 2015). The second group shows $\delta^{13}C_{Carb}$ values between -12 to -20 ‰ (Fig. 5b). This ^{12}C depletion is typical of carbonates formed as a result of the anaerobic oxidation of methane once this methane reaches the zone where it occurs in concert with sulfate (Sivan et al., 2007; Whiticar & Faber, 1986). Authigenic carbonates (C_{auth}) formed as a result of this process may act as a carbon sink, preventing the methane from returning carbon to the ocean, and locking it into stable carbonate phases (Schrag et al., 2013). Previous work in the region has shown widespread evidence for C_{auth} in Bering sediment (Pierre et al., 2016), with similarly ^{12}C-depleted carbon isotope signatures (Hein et al., 1979). As we see little evidence for C_{auth} formation in sediments, and with previous work showing C_{auth} in tephra layers (Hein et al., 1979), it is possible tephra alteration has acted to supply the Ca^{2+} and Mg^{2+} necessary for formation. If true, this would suggest C_{auth} formation is a carbon sink enhanced by tephra diagenesis.

It is also possible tephra deposition may stimulate phytoplankton productivity in surface seawater (Langmann et al., 2010; Olgun et al., 2011). Using both OC content and biogenic barium flux (Ba_{Bio}) as proxies for palaeoproductivity (Schoepfer et al., 2015), we investigated the impact of tephra deposition on productivity in the Bering Sea. There is little evidence of increased productivity in sediments directly surrounding tephra deposits, with slightly lower average OC content, and similar Ba_{Bio} (Fig. 2c). This is despite evidence of plankton blooms in the aftermath of eruptions in the region (Hamme et al., 2010; Langmann et al., 2010). This suggests either that: i) plankton blooms are transitory and short-lived, having very little impact on overall productivity in the region; or ii) the organic carbon produced by such blooms is either not exported from the upper ocean prior to remineralisation, or transported to other locations by ocean currents. In addition, the Bering Sea is

typically an area of high productivity (Wehrmann et al., 2011), so that the addition of tephra makes little difference to overall production. A final possibility is that the andesitic and low-Fe nature of the tephra means insufficient nutrient supply occurs when tephra is deposited.

5 Conclusions

Our results demonstrate enhanced OC preservation in tephra, and in the sediments surrounding tephra deposits. The OC in the tephra layers is primarily associated with reactive metal phases, with an average $f_{OC\text{-}Fe}$ value of 77% in tephra. Thus, tephra layers contain the highest $f_{OC\text{-}Fe}$ proportions yet reported. Isotopic analyses indicate that this OC is primarily marine in origin, supporting previous studies which demostrate the affiliation of Fe_R to marine OC in marine environments (Sirois et al., 2018; Zhao et al., 2018), but with a potentially important contribution from microbial OC. The data also shows the viability of long-term stability of such relationships, with high $f_{OC\text{-}Fe}$ proportions in sediments older than 700 kyr. This finding may explain observed increases in OC activation energy as age increases (Hemingway et al., 2019), with OC-Fe_R interactions resulting in hard to break down organic compounds. In addition to complexation of OC with reactive metal phases, there is limited evidence for authigenic carbonate formation in these tephra layers.

6 References

Achterberg, E. P., Moore, C. M., Henson, S. A., Steigenberger, S., Stohl, A., Eckhardt, S., et al. (2013). Natural iron fertilization by the Eyjafjallajökull volcanic eruption. *Geophysical Research Letters*, *40*(5), 921–926. https://doi.org/10.1002/grl.50221

Arndt, S., Jørgensen, B. B., LaRowe, D. E., Middelburg, J. J., Pancost, R. D., & Regnier, P. (2013). Quantifying the degradation of organic matter in marine sediments: A review and synthesis. *Earth-Science Reviews*, *123*, 53–86. https://doi.org/10.1016/J.EARSCIREV.2013.02.008

Barber, A., Lalonde, K., Mucci, A., & Gélinas, Y. (2014). The role of iron in the diagenesis of organic carbon and nitrogen in sediments: A long-term incubation experiment. *Marine Chemistry*, *162*, 1–9. https://doi.org/10.1016/j.marchem.2014.02.007

Barber, A., Brandes, J., Leri, A., Lalonde, K., Balind, K., Wirick, S., et al. (2017). Preservation of organic matter in marine sediments by inner-sphere interactions with reactive iron. *Scientific Reports*, *7*(1), 366. https://doi.org/10.1038/s41598-017-00494-0

Buggisch, W., Joachimski, M. M., Lehnert, O., Bergström, S. M., Repetski, J. E., & Webers, G. F. (2010). Did intense volcanism trigger the first Late Ordovician icehouse? *Geology*, *38*(4), 327–330. https://doi.org/10.1130/G30577.1

Burdige, D. J. (2007). Preservation of organic matter in marine sediments: Controls, mechanisms, and an imbalance in sediment organic carbon budgets? *Chemical Reviews*, *107*(2), 467–485. https://doi.org/10.1021/cr050347q

Cashman, K. V., Stephen, R., & Sparks, J. (2013). How volcanoes work: A 25 year perspective. *Bulletin of the Geological Society of America*, *125*(5–6), 664–690. https://doi.org/10.1130/B30720.1

Cifuentes, L. A., & Salata, G. G. (2001). Significance of carbon isotope discrimination between bulk carbon and extracted phospholipid fatty acids in selected terrestrial and marine environments. *Organic Geochemistry*, *32*(4), 613–621. https://doi.org/10.1016/S0146-6380(00)00198-4

Coker, V. S., Byrne, J. M., Telling, N. D., Van Der Laan, G., Lloyd, J. R., Hitchcock, A. P., et al. (2012). Characterisation of the dissimilatory reduction of Fe(III)-oxyhydroxide at the microbe - mineral interface: The application of STXM-XMCD. *Geobiology*, *10*(4), 347–354. https://doi.org/10.1111/j.1472-4669.2012.00329.x

Dingwell, D. B., Lavallée, Y., & Kueppers, U. (2012). Volcanic ash: A primary agent in the Earth system. *Physics and Chemistry of the Earth, Parts A/B/C*, *45–46*, 2–4. https://doi.org/10.1016/J.PCE.2011.07.007

Duggen, S., Olgun, N., Croot, P., Hoffmann, L., Dietze, H., Delmelle, P., & Teschner, C. (2010). The role of airborne volcanic ash for the surface ocean biogeochemical iron-cycle: a review. *Biogeosciences*, *7*(3), 827–844. https://doi.org/10.5194/bg-7-827-2010

Elizabeth Cooper, R., Eusterhues, K., Wegner, C. E., Uwe Totsche, K., & Küsel, K. (2017). Ferrihydrite-associated organic matter (OM) stimulates reduction by Shewanella oneidensis MR-1 and a complex microbial consortia. *Biogeosciences*, *14*(22), 5171–5188. https://doi.org/10.5194/bg-14-5171-2017

Eusterhues, K., Hädrich, A., Neidhardt, J., Küsel, K., Keller, T. F., Jandt, K. D., & Totsche, K. U. (2014). Reduction of ferrihydrite with adsorbed and coprecipitated organic matter: Microbial reduction by Geobacter bremensis vs. abiotic reduction by Na-dithionite. *Biogeosciences*, *11*(18), 4953–4966. https://doi.org/10.5194/bg-11-4953-2014

Faust, J. C., Tessin, A., Fisher, B. J., Zindorf, M., Papadaki, S., Hendry, K. R., et al. (2021). Millennial scale persistence of organic carbon bound to iron in Arctic marine sediments. *Nature Communications*, *12*(1), 1–9. https://doi.org/10.1038/s41467-020-20550-0

Fisher, B. J., Moore, O. W., Faust, J. C., Peacock, C. L., & März, C. (2020). Experimental evaluation of the extractability of iron bound organic carbon in sediments as a function of carboxyl content. *Chemical Geology*, *556*, 119853. https://doi.org/10.1016/j.chemgeo.2020.119853

Fisk, M. R., Giovannoni, S. J., & Thorseth, I. H. (1998). Alteration of oceanic volcanic glass: Textural evidence of microbial activity. *Science*, *281*(5379), 978–980. https://doi.org/10.1126/science.281.5379.978

Frogner, P., Reynir Gíslason, S., & Óskarsson, N. (2001). Fertilizing potential of volcanic ash in ocean surface water. *Geology*, *29*(6), 487. https://doi.org/10.1130/0091-7613(2001)029<0487:FPOVAI>2.0.CO;2

Gong, C., & Hollander, D. J. (1997). Differential contribution of bacteria to sedimentary organic matter in oxic and anoxic environments, Santa Monica Basin, California. In *Organic Geochemistry* (Vol. 26, pp. 545–563). Pergamon. https://doi.org/10.1016/S0146-6380(97)00018-1

Hamme, R. C., Webley, P. W., Crawford, W. R., Whitney, F. A., DeGrandpre, M. D., Emerson, S. R.,

et al. (2010). Volcanic ash fuels anomalous plankton bloom in subarctic northeast Pacific. *Geophysical Research Letters*, *37*(19), n/a-n/a. https://doi.org/10.1029/2010GL044629

Hayes, J. M. (2001). Fractionation of carbon and hydrogen isotopes in biosynthetic processes. *Reviews in Mineralogy and Geochemistry*, *43*(1), 191–277. https://doi.org/10.2138/gsrmg.43.1.225

Hedges, J. I., Keil, R. G., & Benner, R. (1997). What happens to terrestrial organic matter in the ocean? In *Organic Geochemistry* (Vol. 27, pp. 195–212). Pergamon. https://doi.org/10.1016/S0146-6380(97)00066-1

Hedges, John I., & Keil, R. G. (1995). Sedimentary organic matter preservation: an assessment and speculative synthesis. *Marine Chemistry*, *49*(2–3), 81–115. https://doi.org/10.1016/0304-4203(95)00008-F

Hein, J. R., O'Neil, J. R., Jones, O'NEIL, J. R., & JONES, M. G. (1979). Origin of authigenic carbonates in sediment from the deep Bering Sea. *Sedimentology*, *26*(5), 681–705. https://doi.org/10.1111/j.1365-3091.1979.tb00937.x

Hembury, D. J., Palmer, M. R., Fones, G. R., Mills, R. A., Marsh, R., & Jones, M. T. (2012). Uptake of dissolved oxygen during marine diagenesis of fresh volcanic material. *Geochimica et Cosmochimica Acta*, *84*, 353–368. https://doi.org/10.1016/J.GCA.2012.01.017

Hemingway, J. D., Rothman, D. H., Grant, K. E., Rosengard, S. Z., Eglinton, T. I., Derry, L. A., & Galy, V. V. (2019). Mineral protection regulates long-term global preservation of natural organic carbon. *Nature*, *570*(7760), 228–231. https://doi.org/10.1038/s41586-019-1280-6

Homoky, W. B., Hembury, D. J., Hepburn, L. E., Mills, R. A., Statham, P. J., Fones, G. R., & Palmer, M. R. (2011). Iron and manganese diagenesis in deep sea volcanogenic sediments and the origins of pore water colloids. *Geochimica et Cosmochimica Acta*, *75*(17), 5032–5048. https://doi.org/10.1016/J.GCA.2011.06.019

Humphreys, M. P., Achterberg, E. P., Griffiths, A. M., McDonald, A., & Boyce, A. J. (2015).

436 Measurements of the stable carbon isotope composition of dissolved inorganic carbon in the
437 northeastern Atlantic and Nordic Seas during summer 2012. *Earth System Science Data*, *7*(1),
438 127–135. https://doi.org/10.5194/essd-7-127-2015

439 Jones, M. T., & Gislason, S. R. (2008). Rapid releases of metal salts and nutrients following the
440 deposition of volcanic ash into aqueous environments. *Geochimica et Cosmochimica Acta*,
441 *72*(15), 3661–3680. https://doi.org/10.1016/j.gca.2008.05.030

442 Kato, S., Nakamura, R., Kai, F., Watanabe, K., & Hashimoto, K. (2010). Respiratory interactions of
443 soil bacteria with (semi)conductive iron-oxide minerals. *Environmental Microbiology*, *12*(12),
444 3114–3123. https://doi.org/10.1111/j.1462-2920.2010.02284.x

445 Kostka, J. E., & Luther, G. W. (1994). Partitioning and speciation of solid phase iron in saltmarsh
446 sediments. *Geochimica et Cosmochimica Acta*, *58*(7), 1701–1710. https://doi.org/10.1016/0016-
447 7037(94)90531-2

448 Lalonde, K., Mucci, A., Ouellet, A., & Gélinas, Y. (2012). Preservation of organic matter in
449 sediments promoted by iron. *Nature*, *483*(7388), 198–200. https://doi.org/10.1038/nature10855

450 Langmann, B., Zakšek, K., Hort, M., & Duggen, S. (2010). Volcanic ash as fertiliser for the surface
451 ocean. *Atmos. Chem. Phys. Atmospheric Chemistry and Physics*, *10*, 3891–3899. Retrieved from
452 www.atmos-chem-phys.net/10/3891/2010/

453 LaRowe, D. E., Arndt, S., Bradley, J. A., Estes, E. R., Hoarfrost, A., Lang, S. Q., et al. (2020, May 1).
454 The fate of organic carbon in marine sediments - New insights from recent data and analysis.
455 *Earth-Science Reviews*. Elsevier B.V. https://doi.org/10.1016/j.earscirev.2020.103146

456 Lee, C.-T. A., Jiang, H., Ronay, E., Minisini, D., Stiles, J., & Neal, M. (2018). Volcanic ash as a
457 driver of enhanced organic carbon burial in the Cretaceous. *Scientific Reports*, *8*(1), 4197.
458 https://doi.org/10.1038/s41598-018-22576-3

459 Li, L., Bai, S., Li, J., Wang, S., Tang, L., Dasgupta, S., et al. (2020). Volcanic ash inputs enhance the
460 deep-sea seabed metal-biogeochemical cycle: A case study in the Yap Trench, western Pacific

Ocean. *Marine Geology*, *430*, 106340. https://doi.org/10.1016/j.margeo.2020.106340

Longman, J., Palmer, M. R., Gernon, T. M., & Manners, H. R. (2019). The role of tephra in enhancing organic carbon preservation in marine sediments. *Earth-Science Reviews*, *192*, 480–490. https://doi.org/10.1016/j.earscirev.2019.03.018

Longman, J., Palmer, M. R., & Gernon, T. M. (2020). Viability of greenhouse gas removal via artificial addition of volcanic ash to the ocean. *Anthropocene*, *32*. https://doi.org/10.1016/j.ancene.2020.100264

Luo, M., Torres, M. E., Hong, W. L., Pape, T., Fronzek, J., Kutterolf, S., et al. (2020). Impact of iron release by volcanic ash alteration on carbon cycling in sediments of the northern Hikurangi margin. *Earth and Planetary Science Letters*, *541*, 116288. https://doi.org/10.1016/j.epsl.2020.116288

Maters, E. C., Delmelle, P., & Gunnlaugsson, H. P. (2017). Controls on iron mobilisation from volcanic ash at low pH: Insights from dissolution experiments and Mössbauer spectroscopy. *Chemical Geology*, *449*, 73–81. https://doi.org/10.1016/J.CHEMGEO.2016.11.036

Mehra, O. P., & Jackson, M. L. (1958). Iron Oxide Removal from Soils and Clays by a Dithionite-Citrate System Buffered with Sodium Bicarbonate. *Clays and Clay Minerals*, *7*(1), 317–327. https://doi.org/10.1346/CCMN.1958.0070122

Moore, C. M., Mills, M. M., Arrigo, K. R., Berman-Frank, I., Bopp, L., Boyd, P. W., et al. (2013). Processes and patterns of oceanic nutrient limitation. *Nature Geoscience*, *6*(9), 701–710. https://doi.org/10.1038/ngeo1765

Muratli, J. M., McManus, J., Mix, A., & Chase, Z. (2012). Dissolution of fluoride complexes following microwave-assisted hydrofluoric acid digestion of marine sediments. *Talanta*, *89*, 195–200. https://doi.org/10.1016/j.talanta.2011.11.081

Murray, N.A., Muratli, J. M., Hartwell, A. M., Manners, H., Megowan, M. R., Goñi, M., et al. (2016). Data report: dissolved minor element compositions, sediment major and minor element

concentrations, and reactive iron and manganese data from the Lesser Antilles volcanic arc region, IODP Expedition 340 Sites U1394, U1395, U1396, U1399, and U1400. *Proceedings of the Integrated Ocean Drilling Program*, *340*. https://doi.org/10.2204/iodp.proc.340.207.2016

Murray, Natalie A., McManus, J., Palmer, M. R., Haley, B., & Manners, H. (2018). Diagenesis in tephra-rich sediments from the Lesser Antilles Volcanic Arc: Pore fluid constraints. *Geochimica et Cosmochimica Acta*, *228*, 119–135. https://doi.org/10.1016/J.GCA.2018.02.039

Olgun, N., Duggen, S., Croot, P. L., Delmelle, P., Dietze, H., Schacht, U., et al. (2011). Surface ocean iron fertilization: The role of airborne volcanic ash from subduction zone and hot spot volcanoes and related iron fluxes into the Pacific Ocean. *Global Biogeochemical Cycles*, *25*(4), n/a-n/a. https://doi.org/10.1029/2009GB003761

Pierre, C., Blanc-Valleron, M. M., Caquineau, S., März, C., Ravelo, A. C., Takahashi, K., & Alvarez Zarikian, C. (2016). Mineralogical, geochemical and isotopic characterization of authigenic carbonates from the methane-bearing sediments of the Bering Sea continental margin (IODP Expedition 323, Sites U1343-U1345). *Deep-Sea Research Part II: Topical Studies in Oceanography*, *125–126*, 133–144. https://doi.org/10.1016/j.dsr2.2014.03.011

Pyle, D. M. (1989). The thickness, volume and grainsize of tephra fall deposits. *Bulletin of Volcanology*, *51*(1), 1–15. https://doi.org/10.1007/BF01086757

Pyle, D. M. (1995). Mass and energy budgets of explosive volcanic eruptions. *Geophysical Research Letters*, *22*(5), 563–566. https://doi.org/10.1029/95GL00052

Roy, M., McManus, J., Goñi, M. A., Chase, Z., Borgeld, J. C., Wheatcroft, R. A., et al. (2013). Reactive iron and manganese distributions in seabed sediments near small mountainous rivers off Oregon and California (USA). *Continental Shelf Research*, *54*, 67–79. https://doi.org/10.1016/J.CSR.2012.12.012

Schoepfer, S. D., Shen, J., Wei, H., Tyson, R. V., Ingall, E., & Algeo, T. J. (2015). Total organic carbon, organic phosphorus, and biogenic barium fluxes as proxies for paleomarine productivity.

Earth-Science Reviews, *149*, 23–52. https://doi.org/10.1016/J.EARSCIREV.2014.08.017

Schrag, D. P., Higgins, J. A., Macdonald, F. A., & Johnston, D. T. (2013). Authigenic carbonate and the history of the global carbon cycle. *Science*, *339*(6119), 540–3. https://doi.org/10.1126/science.1229578

Scudder, R. P., Murray, R. W., & Plank, T. (2009). Dispersed ash in deeply buried sediment from the northwest Pacific Ocean: An example from the Izu–Bonin arc (ODP Site 1149). *Earth and Planetary Science Letters*, *284*(3–4), 639–648. https://doi.org/10.1016/J.EPSL.2009.05.037

Shields, M. R., Bianchi, T. S., Gélinas, Y., Allison, M. A., & Twilley, R. R. (2016). Enhanced terrestrial carbon preservation promoted by reactive iron in deltaic sediments. *Geophysical Research Letters*, *43*(3), 1149–1157. https://doi.org/10.1002/2015GL067388

Sirois, M., Couturier, M., Barber, A., Gélinas, Y., & Chaillou, G. (2018). Interactions between iron and organic carbon in a sandy beach subterranean estuary. *Marine Chemistry*. https://doi.org/10.1016/J.MARCHEM.2018.02.004

Sivan, O., Schrag, D. P., & Murray, R. W. (2007). Rates of methanogenesis and methanotrophy in deep-sea sediments. *Geobiology*, *5*, 141–151. https://doi.org/10.1111/j.1472-4669.2007.00098.x

Staudigel, H., Furnes, H., McLoughlin, N., Banerjee, N. R., Connell, L. B., & Templeton, A. (2008, August 1). 3.5 billion years of glass bioalteration: Volcanic rocks as a basis for microbial life? *Earth-Science Reviews*. Elsevier. https://doi.org/10.1016/j.earscirev.2008.04.005

Straub, S. M., & Schmincke, H. U. (1998). Evaluating the tephra input into Pacific Ocean sediments: distribution in space and time. *Geologische Rundschau*, *87*(3), 461–476. https://doi.org/10.1007/s005310050222

Takahashi, K., Ravelo, A., & Alvarez-Zarikian, C. (2011). *Proceedings of the Integrated Ocean Drilling Program: Expedition Reports: Bering Sea Paleoceanography. vol. 323*. College Station, Texas: Integrated Ocean Drilling Program Management International, Inc., for the Integrated Ocean Drilling Program.

536 Takahashi, K., Ravelo, A. C., & Alvarez Zarikian, C. A. (2011). Site U1339. In *Proceedings of the*
537 *Integrated Ocean Drilling Program Volume 323* (p. 84). Tokyo: Integrated Ocean Drilling
538 Program Management International, Inc.

539 Tang, L., Song, Y., Jiang, S., Jiang, Z., Li, Z., Yang, Y., et al. (2020). Organic matter accumulation of
540 the Wufeng-Longmaxi shales in southern Sichuan Basin: Evidence and insight from volcanism.
541 *Marine and Petroleum Geology*, *120*, 104564. https://doi.org/10.1016/j.marpetgeo.2020.104564

542 Thorseth, I. H., Furnes, H., & Tumyr, O. (1995). Textural and chemical effects of bacterial activity on
543 basaltic glass: an experimental approach. *Chemical Geology*, *119*(1–4), 139–160. https://doi.org/
544 10.1016/0009-2541(94)00098-S

545 Thorseth, I. H., Torsvik, T., Torsvik, V., Daae, F. L., & Pedersen, R. B. (2001). Diversity of life in
546 ocean floor basalt. *Earth and Planetary Science Letters*, *194*(1–2), 31–37.
547 https://doi.org/10.1016/S0012-821X(01)00537-4

548 Uematsu, M., Toratani, M., Kajino, M., Narita, Y., Senga, Y., & Kimoto, T. (2004). Enhancement of
549 primary productivity in the western North Pacific caused by the eruption of the Miyake-jima
550 Volcano. *Geophysical Research Letters*, *31*(6), n/a-n/a. https://doi.org/10.1029/2003gl018790

551 Vaughn, D. R., & Caissie, B. E. (2017). Effects of sea-level, sea-ice extent, and nutrient availability
552 on primary production at the Umnak Plateau, Bering Sea (IODP Site U1339) during Marine
553 Isotope Stage (MIS) 5. *Palaeogeography, Palaeoclimatology, Palaeoecology*, *485*, 283–292.
554 https://doi.org/10.1016/J.PALAEO.2017.06.020

555 Wagai, R., & Mayer, L. M. (2007). Sorptive stabilization of organic matter in soils by hydrous iron
556 oxides. *Geochimica et Cosmochimica Acta*, *71*(1), 25–35.
557 https://doi.org/10.1016/j.gca.2006.08.047

558 Wallmann, K., Aloisi, G., Haeckel, M., Tishchenko, P., Pavlova, G., Greinert, J., et al. (2008). Silicate
559 weathering in anoxic marine sediments. *Geochimica et Cosmochimica Acta*, *72*(12), 2895–2918.
560 https://doi.org/10.1016/j.gca.2008.03.026

Wehrmann, L. M., Risgaard-Petersen, N., Schrum, H. N., Walsh, E. A., Huh, Y., Ikehara, M., et al. (2011). Coupled organic and inorganic carbon cycling in the deep subseafloor sediment of the northeastern Bering Sea Slope (IODP Exp. 323). *Chemical Geology*, *284*(3–4), 251–261. https://doi.org/10.1016/j.chemgeo.2011.03.002

Whiticar, M. J., & Faber, E. (1986). Methane oxidation in sediment and water column environments —Isotope evidence. *Organic Geochemistry*, *10*(4–6), 759–768. https://doi.org/10.1016/S0146-6380(86)80013-4

Zhang, R., Jiang, T., Tian, Y., Xie, S., Zhou, L., Li, Q., & Jiao, N. (2017). Volcanic ash stimulates growth of marine autotrophic and heterotrophic microorganisms. *Geology*, *45*(8), G38833.1. https://doi.org/10.1130/G38833.1

Zhao, B., Yao, P., Bianchi, T. S., Shields, M. R., Cui, X. Q., Zhang, X. W., et al. (2018). The Role of Reactive Iron in the Preservation of Terrestrial Organic Carbon in Estuarine Sediments. *Journal of Geophysical Research: Biogeosciences*, *123*(12), 3556–3569. https://doi.org/10.1029/2018JG004649

7 Acknowledgements

This work was funded by NERC grant NE/K00543X/1, “The role of marine diagenesis of tephra in the carbon cycle”. Datasets for this research are available in the Supplementary Information, and on the Pangaea data archive (doi to follow once assigned)

8 Figures

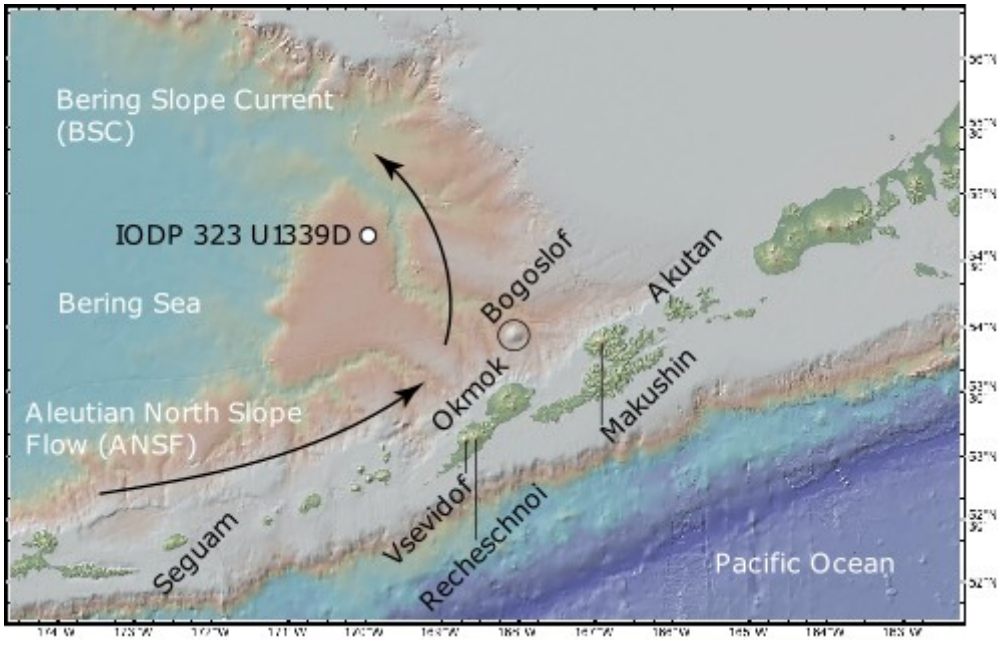

Figure 1: Location map of part of the Aleutian Island Arc showing the location of IODP core U1339D. Also indicated is a number of volcanoes which have actively supplied ash to the Bering Sea over the Quaternary Period (as defined by the Global Volcanism Program of the Smithsonian Institution).

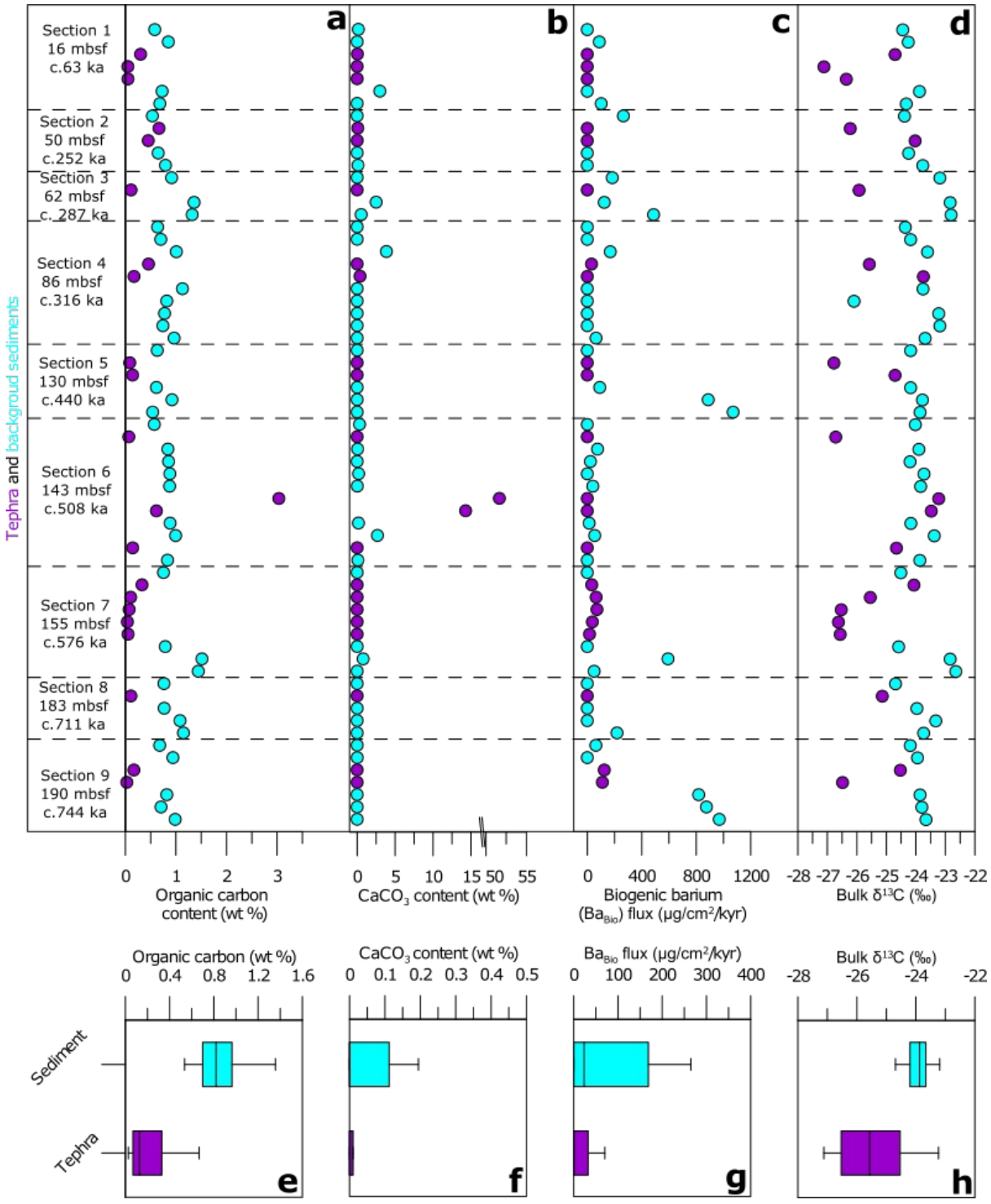

588

589 Figure 2: Geochemical parameters of tephra and background sediment from U1339D. a) Organic
590 carbon content in tephra (purple) and background sediments (blue). b) $CaCO_3$ content, c) biogenic
591 barium flux, d) bulk $\delta^{13}C$, with average value for both sample type indicated by solid lines. To the left
592 of boxes a-d are the section numbers, depths in metres below sea floor (mbsf) and indicative ages in
593 thousands of years before present (ka). Panels e-h display box and whisker diagrams of the data

presented in panels a-d. Boxes are defined between the first and third quartile (interquartile range; IQR), with minimum and maximum whiskers representative of 1.5 times the IQR, and with outliers (>1.5 times IQR) removed.

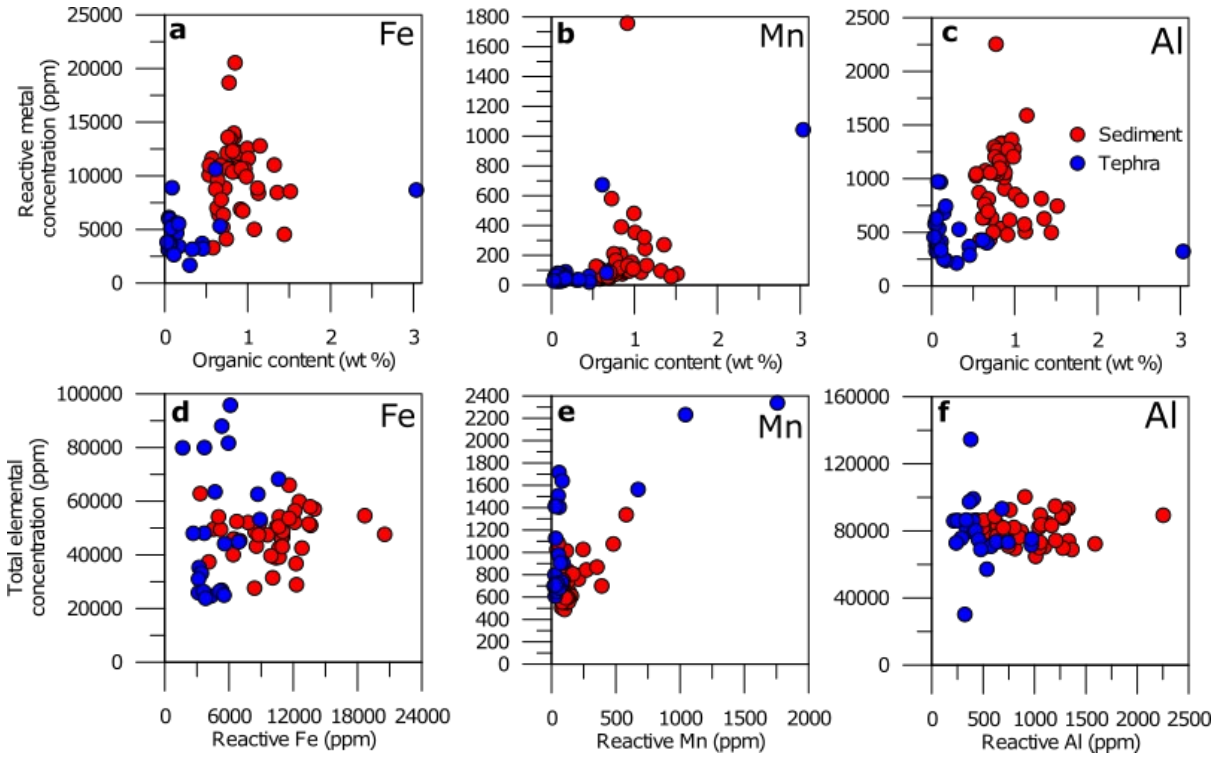

Figure 3: Comparison of total metal contents, reactive metal contents and organic carbon (OC) content of sediments and tephras from Site U1339D. Panels a-c display reactive metal concentrations plotted against OC whilst panels d-f show total elemental content for Fe, Mn and Al against respective reactive metal content. Tephra samples are coloured blue, with sediments in red.

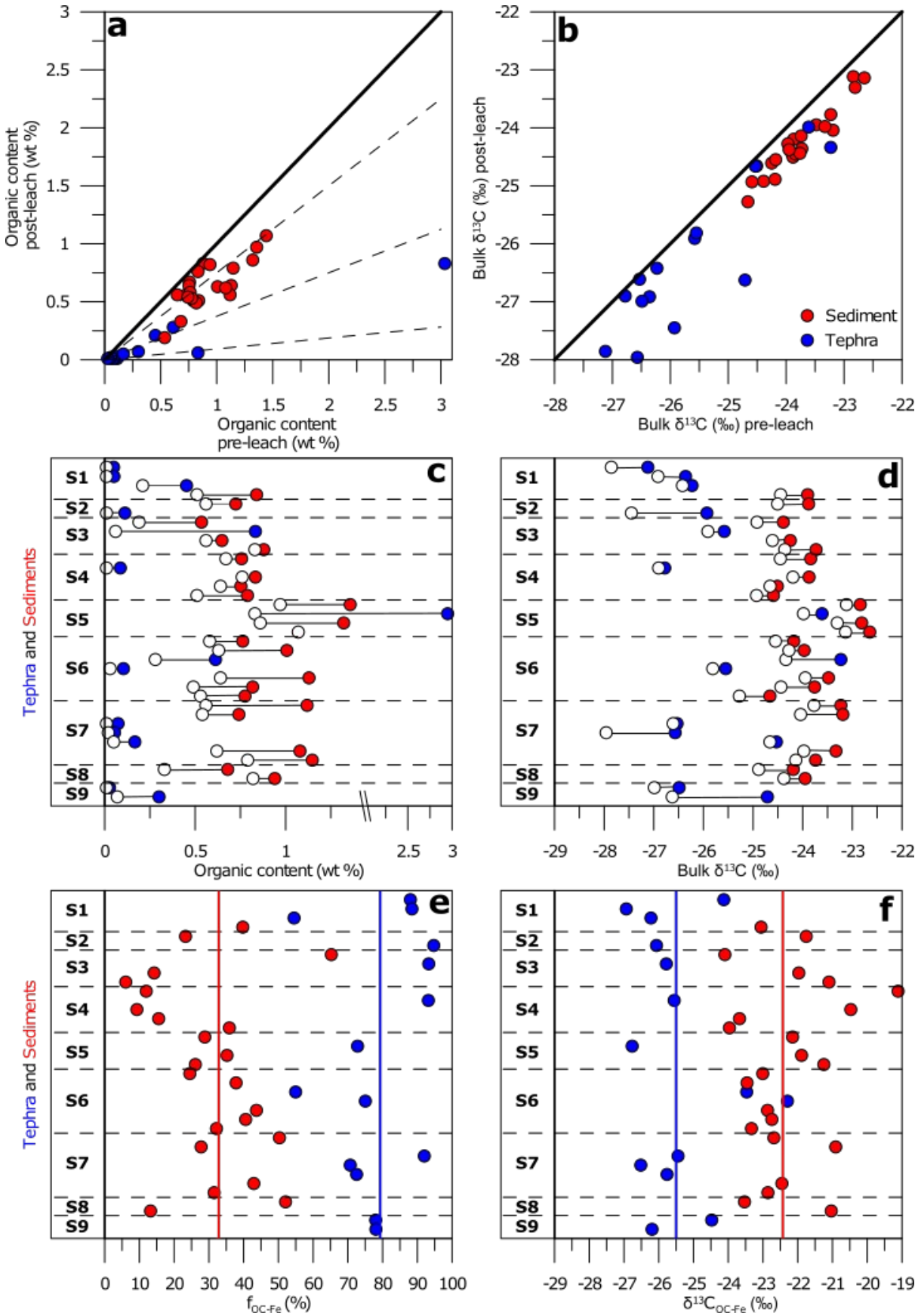
a
Organic content post-leach (wt %)
Organic content pre-leach (wt %)
b
Bulk δ13C (‰) post-leach
Bulk δ13C (‰) pre-leach
Sediment
Tephra
c
Tephra and Sediments
Organic content (wt %)
d
Bulk δ13C (‰)
e
fOC-Fe (%)
f
δ13COC-Fe (‰)
S1
S2
S3
S4
S5
S6
S7
S8
S9

602

Figure 4: Results of dithionite extraction experiments. In all panels, tephras are indicated by blue circles and background sediments are in red. a) Organic carbon (OC) content in all samples before extraction versus OC content after extraction. Thick black line indicates where samples should plot if no OC was extracted. Labelled dashed lines indicate the fraction of OC associated with reactive phases ($f_{OC\text{-}Fe}$). b) Plot of bulk $\delta^{13}C$ before and after extraction. Thick black line indicates where samples should plot if no isotopic change were observed. Panels c-d display the same data as a and b but indicate the shift from the original sample (filled circles) to extracted samples (open circles). e) $f_{OC\text{-}Fe}$, with thick lines indicating average $f_{OC\text{-}Fe}$ for tephra (blue) and sediment (red). f) Bulk isotopic composition of OC associated with reactive phases $\delta^{13}C_{OC\text{-}Fe}$. As before, thick coloured lines indicate the average $\delta^{13}C_{OC\text{-}Fe}$ of tephra (blue) and sediments (red). For panels c-f, section numbers are indicated to the left. These refer to the ages and depths indicated in Figure 2.

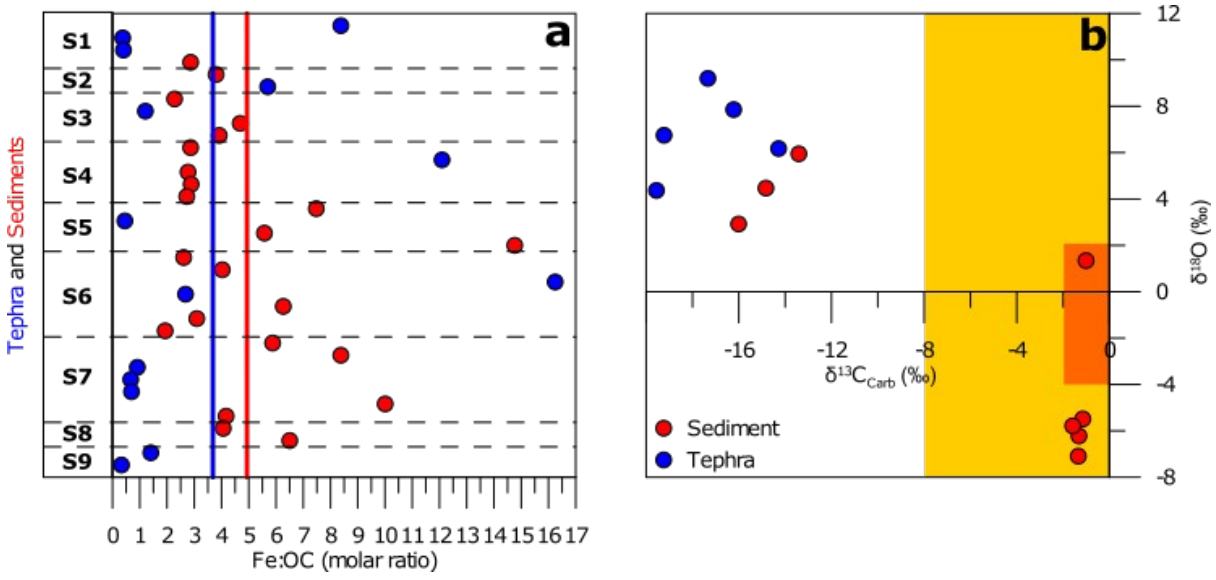

Figure 5: Geochemistry of tephras and sediments from Site U1339D. a) Ratio of reactive Fe (FeR) to OC, using molar masses for sediments (red) and tephra (blue). b) $\delta^{13}C$ and $\delta^{18}O$ of the carbonate fraction (see Methods), with typical values for isotopic composition of seawater (orange rectangle) and biogenic carbonate (yellow rectangle) highlighted. For panel a, section numbers are indicated to the left. These refer to the ages and depths indicated in Figure 2.

9 Tables

Table 1: Summary of experimental results. Mean, minimum and maximum values for each of the measured variable are presented, for both tephra and sediment layers.

Tephra Layers			
	Mean	Minimum	Maximum
Before dithionite extraction			
Organic carbon content (wt%)	0.33	0.03	3.03
Inorganic carbon content (wt%)	3.02	0	51.66
Ba_{Bio} flux (mg cm^{-3} kyr)	201	0	2682
Total Fe (wt%)	4.8	2.38	9.58
Total Mn (ppm)	1082	608	2232
Total Al (wt%)	7.98	3.02	13.4
Bulk $\delta^{13}C$ (‰)	-25.4	-23.23	-27.12
After dithionite extraction			
Organic carbon content (wt%)	0.12	0.01	0.83
Reactive Fe (wt %)	0.57	0.32	1.06
Reactive Mn (ppm)	175	19.83	1042
Reactive Al (ppm)	524.92	287.8	972.8
Bulk $\delta^{13}C$ (‰)	-26.29	-23.99	-27.96
$f_{Fe\text{-}OC}$ (%)	0.79	0.55	0.95
$\delta^{13}C_{Fe\text{-}OC}$ (%)	-25.83	-23.39	-24.16
Sediment Layers			
	Mean	Minimum	Maximum
Before dithionite extraction			
Organic carbon content (wt%)	0.84	0.15	1.41
Inorganic carbon content (wt%)	0.33	0	3.86
Ba_{Bio} flux (mg cm^{-3} kyr)	166	0	1071
Total Fe (wt%)	4.8	2.88	6.6
Total Mn (ppm)	784.8	488.4	2337
Total Al (wt%)	8.04	6.47	10.03
Bulk $\delta^{13}C$ (‰)	-23.82	-22.65	-24.71
After dithionite extraction			
Organic carbon content (wt%)	0.61	0.07	1.07
Reactive Fe (wt %)	0.98	0.17	1.87
Reactive Mn (ppm)	170.8	34.32	580.5
Reactive Al (ppm)	914.42	214.4	2254
Bulk $\delta^{13}C$ (‰)	-24.37	-23.99	-27.96
$f_{Fe\text{-}OC}$ (%)	0.33	0.06	0.78
$\delta^{13}C_{Fe\text{-}OC}$ (%)	-24.16	-22.94	-26.39